FULL-SCALE AIRCRAFT TIRE PRESSURE TESTS

C. Fabre
AIRBUS S.A.S, France
Cyril.fabre@airbus.com

JM. Balay
LCPC, France
Jean-maurice.balay@lcpc.fr

P. Lerat
DGAC, France
Patrick.lerat@aviation-civile.gouv.fr

Presented for the
2010 FAA Worldwide Airport Technology Transfer Conference
Atlantic City, NJ
20-22 April 2010

ABSTRACT: This paper describes an outdoor full-scale test led by Airbus S.A.S in partnership with the French authorities DGAC-STAC, LCPC, LRPC-T, MICHELIN and VANCOUVER² to improve experimental and theoretical knowledge related to the effects of aircraft internal tire inflation pressure on the behavior of and damage to flexible pavement. Since some modern aircraft have tire pressures exceeding 15 bar, the tests focus on pressures from 15 bar to 17.5 bar. The experimental pavement located on the Toulouse-Blagnac airport in France includes up to seven different test sections, representative of current airfield flexible pavement worldwide. Variant parameters from one section to another are thickness of AC surface layer and its performance in respect of rutting, and surface treatment as grooving. The aircraft simulation vehicle drives four dual-wheel gears sufficiently spaced enough in order to prevent from any interaction between them, making it possible to test two different tire pressures (15 and 17.5 bar) and two weights per wheel (ultimate weights, 28.5 and 33.2 tons) simultaneously. The seven test sections are instrumented to measure resilient strains, and resilient and permanent displacements (rutting). The structure has been initially designed according to the French airport pavement design method, for 10,000 passes of B747-400 gear. Tests will continue until the simulator runs are no longer possible due to the high rut depth level.

KEY WORDS: Pavement, tire pressure, rutting, full-scale tests.

1. INTRODUCTION

The PCN number is mainly driven by the bearing capacity of two types of pavement (flexible and rigid) and for four levels of pavement strength (characterized by the CBR for flexible pavement at the top of subgrade, and by the K-modulus for rigid pavement at the bottom of the slab).
In addition, a third code associated to the PCN represents tire pressure limitation:

W = No pressure limitation
X = 15 bar limitation
Y = 10 bar limitation
Z = 5 bar limitation.

High-tire pressure limitation was initially established by the Australian Air force to prevent damage to asphalt surface runways used by military aircraft with high tire pressure (around 20 bars or more). Later these limitations have been extended to commercial operations regulation.
New generation aircraft (B787/B777/A340/A380 etc.) tend to increase the load per wheel therefore internal tire pressure inflation, above 16 bar in some cases. The current scale of maximum allowed tire pressure is not technically substantiated and not representative of current aircraft with higher gross weights and higher tire pressures.
In order to assess the real tire pressure influence on asphalt surface layers, Airbus proposes to carryout a full-scale test campaign by using the Pavement experimental vehicle simulator (Turtle) developed formerly in the framework of the AIRBUS Experimental Programs to be used on seven instrumented flexible pavement sections.
The main goal of this research is to study the influence of internal tire pressure inflation in respect to the permanent deformation (rutting) created by traffic at the surface asphaltic material. The second objective is to collect data on flexible pavement material behavior in regard to heavy loads application (this data will complete the A380 PEP [Pavement Experimental Program] database). In order to achieve these objectives, the experimental pavement will be equipped with various sensors, which will be installed both during the experimental pavement construction and after its completion. The L/G (landing gear) simulator used during the PEP will operate over the whole length of the pavement. To reproduce the distress of pavement asphalt layers due to new generation airplane such A380 or B777, it is anticipated that the simulator will make between 10,000 and 15,000 passes over the pavement.

2. BACKGROUND

In the ICAO Annex-14[ref.1] it is stated that: " The PCN reported shall indicate that an aircraft with an ACN number equal to or less than reported PCN can operate on the pavement subject to any limitation on the tire pressure, or aircraft all-up mass for specified aircraft type."
In the ICAO ADM [ref.2], the tire pressure category is considered as follows:
"Directly at the surface the tire contact pressure is the most critical element of loading with little relation to the other aspects of pavement strength. This is the reason for reporting permissible tire pressure in terms of tire pressure categories. Except for rare cases of spalling joints and unusual surface deficiencies, rigid pavements do not require tire pressure restrictions. However, pavements categorized as rigid which have overlays of flexible or bituminous construction must be treated as flexible pavements for reporting permissible tire pressure. Flexible pavements which are classified in the highest tire pressure category must be of very good quality and integrity, while those classified in the lowest category need only be capable of accepting casual highway traffic. It will usually be adequate, except where limitations are obvious, to establish category limits only when experience with high tire pressures indicates pavement distress."

The main high pressure impacts on poor pavement surface quality (generally linked to pressure limitation) are:

- Shear failure: Permanent deformation of a surface or soil due to a load on a relatively small surface area, which then sinks into the surfacing.
- Permanent deformation of the surface, due to the rutting of bituminous materials. Rutting is exacerbated by high AC temperature, low load moving speed and high shear stresses,
- Stripping (maneuvering operations): Failure in bituminous surfacing in which aggregates are dislodged and asphalt binder is lost due to high tangential stress or errors in the laying process.

Airport operators who published their flexible PCN with a code X letter generally have a poor asphalt surface quality. This results in the high-pressure limit.

Consistency of current "allowable tire pressure category"

For main landing gear tires, usual worst case is for static loads at maximum ramp weight (MRW) and maximum aft center of gravity conditions. For nose landing gear tires, usual worst case is for stabilized braking loads at max ramp weight and forward center of gravity conditions.

Worst-case load depends on aircraft landing gear concept e.g.: for multiple gear (A340, B747, A380) max static loads between flat & cambered runway condition. The internal tire pressure inflation is one of the parameters used for ACN calculation including wheel spacing and load per wheel. However, influence of tire pressure in ACN calculation is secondary to load and wheel spacing but tire pressure is heavily influenced by wheel load and tire specifications (ratings, size etc.).

As an example, an aircraft with a heavy wheel load will necessarily have a specific tire with compliant load capabilities, resulting in high tire pressure and a high ACN number due to the heavy wheel load. This is the dilemma of the double penalty: The aircraft is penalized due to its heavy wheel load, i.e. a high ACN, so the aircraft can only operate on runways with high PCN without tire pressure limitation (code W). However, many runways with a relatively high PCN are limited to 15 bar operations (code X) which means the aircraft operation is limited by tire pressure not PCN. For runways with a relatively low PCN and a 15 bar (or less) tire pressure limitation the tire pressure limitation is redundant because aircraft operations are already limited by their ACN exceeding the reported PCN.

3 TEST FACILITIES

3.1 Experimental pavement design.

3.1.1 Capping layer material

The specified material was an Untreated Graded Aggregate 0/20 mm. The objective was to obtain on the finished surface an EV_2modulus[1]>70MPa, a grade tolerance of +/-3 cm for 90% of the controlled points and a mean density >95% Modified Proctor Test index (OPM) for 50% of the controlled points.

3.1.2 Sub-base course material

The specified material was an Untreated Graded Aggregate 0/20mm. The objective was to obtain a mean density > 97.5% OPM (for 50% of the control points), a grade tolerance of +/- 2 cm (for 90% of the control points) and a finished surface with depressions less than 2 cm when measured by a 3 m straight-edge.

3.1.3 Base course material

The specified material was continuous graded 0/14 mm base surface asphalt (EB14-GB). These specifications concerned the quality of manufacturing (control of job mix formula, grading and binder content, air void content, water sensitivity, rutting test, modulus) and the quality of application (minimum temperature of 130°C, grade tolerance of +/- 1cm, slope tolerance of +/- 1cm/m for more than 95% of control points, and surface depressions less than 0.3 cm with a 3m straight-edge for 100% of control points).

3.1.4 Surface course material

The aim of the High Tire Pressure Tests (HTPT) experiment is to test the influence of tire pressure on the characteristics of 3 types of surface asphalt concrete (SAC), when subjected to 10,000 passes of the AIRBUS simulator. The properties of SAC1, SAC2 and SAC3 are given in Table 1.

Surface asphalt concrete type 1 (EB14-BBA C class 3, according the European designation) is the material commonly used in airfield pavement with a required minimum modulus of 7000 MPa. Surface asphalt concrete type 2 (EB14-BB class 3, according the European designation) exhibits higher rutting performances than Surface asphalt concrete type 1. Surface asphalt concrete type 3 (EB14-BB, according the European designation) is sensitive to rutting.

Table 1: Properties of the 3 types of surface asphalt concrete

	Grading	**Specified Bitumen**	**Maximum rutting depth**
Surface asphalt concrete type 1 (EB14-BBA C class 3)	Continuous 0-14mm	35/50 or 50/70	Comprised between 5 et 7.5% deep 10,000 cycles
Surface asphalt concrete type 2 (EB14-BB class 3)	Continuous 0-14mm	50/70	Comprised between 2 et 4% deep 10,000 cycles
Surface asphalt concrete type 3	Continuous 0-14mm	Pure bitumen 50/70 or 70/100	Comprised between 9 et 14% deep 10,000 cycles

As shown in Figure 1, SAC1 is tested on 4 structures (A, B, C and E), with distinct thickness values, evolving from 6 cm to 12 cm. This material is tested as a grooved surface on structure F.
The base asphalt concrete of the 7 sections consists of the material commonly used on civil platforms: EB14-GB class 3 (referred to as BAC) with a thickness fixed at 14cm on structure C, 18 cm on structures B, D, E, F and G and 20 cm on structure A.
The sub-base course, made of 40 cm of UGA and the foundation course and composed of 70 cm of UGA, is common to all the sections.

[1] Young modulus measured by the device Dynaplaque II, according to the French standard NF P 94-117-2

Structure A	Structure B	Structure C	Structure D	Structure E	Structure F	Structure G
0.06m SAC1	0.08m SAC1	0.12m SAC1	0.08m SAC2	0.08m SAC1	0.08m SAC1gr	0.08m SAC3
0.2m BAC	0.18m BAC	0.14m BAC	0.18m BAC	0.18m BAC	0.18m BAC	0.18m BAC
0.4m UGA	0.4m UGA	0.4m UGA	0.4m UGA	0.4m UGA	0.4m UGA	0.4m UGA
0.7m foundation	0.7m foundation	0.7m foundation	0.7m foundation	0.7m foundation	0.7m foundation	0.7m foundation

Figure 1: Pavement materials of the 7 test sections

The contract specifications concerned the quality of manufacturing (control of job mix formula, grading and binder content, air void content, water sensitivity, rutting test, modulus) and the quality of application (minimal temperature of 125°C for SAC1 and 130°C for SAC2 and 3% air void content (Colin White test) mean value in the range 93-97% of the reference density (XP P 98 151), thickness tolerance of +/- 0.5cm for more than 95% of control points, slope tolerance of +/- 0.5cm/m for 100% of control points, surface depressions less than 0.3cm with a 3m straight-edge for 100% of control points).

3.1.5 Update phase: flexible overlay

Experimental pavement was initially designed to support heavy loads representative of current aircraft fleet (and high tire pressure up to 17.5 bar) but it was initially considered as unnecessary to simulate high traffic level since rutting curve is expected to have a logarithmic progression therefore in respect of high tire pressure effect, only the first 2,000 or 3,000 passes need be considered.
However, during the High Tire Pressure Tests Workshop held in Toulouse, France, March 2009, worldwide-recognized attendees requested:
1- to simulate high traffic (between 10,000 and 15,000 passes) to be representative of a 'normal' pavement design life, and to explore the full process of pavement surface damage. This simulation led to re-design the pavement test section accordingly so that premature structural damage could be avoided and test objectives maintained, although some could argue that passes above 3,000 passes is of less interest when considering high tire pressure effects.
As a result of the decision to test the pavement with high traffic level (under heavy loads and pressure, resp. 33.2 t and 17.5 bar), test pavement was re-built by removing the asphalt concrete (AC) surface layer and adding extra base AC course. The new asphalt concrete surface is identical to the previous one, with a new set of additional gauges. This 'base course overlay' is essential to avoid preliminary structural damages when testing pavement with high traffic level.
2- to emulate Australian runways, it was also decided to test pavement in high ambient temperature*s*. Tests will be stopped in July 2010, after a significant number of passes at high temperature (around 55 or 60°C) at pavement surface.
The reinforcement phase consisted in removing the superficial part of the existing pavement by cold micro milling. The specified depth to be removed was comprised between 2 and 5 mm. Using the Alizé software, it was calculated that an additional 21cm asphalt base (EB14-GB) had to be applied in 2 layers (9 cm at the bottom and 12 cm at top) on the overall surface. In that stage, EB14-GB class 4 replaced class 3 EB14-GB. Class 4 EB14-GB is higher resistant than class3 EB14-GB. Compared characteristics are given in Table 2.

Material	Maximal void content	Rutting at 60°C	Complex modulus at 15°C - 10 Hz
Class 3 Base Asphalt Concrete	10% (120 gyrations)	Comprised between 7 et 10% deep at 10,000 cycles	Minimum = 9,000 MPa
Class 4 Base Asphalt Concrete	9% (120 gyrations)	Comprised between 5 et 8% deep at 30,000 cycles	Minimum= 11,000 MPa

Table 2: Compared laboratory characteristics of Class 3 and Class 4 base asphalt concrete

3.2 Simulator vehicle

3.2.1 Specifications

The simulation vehicle has a speed of around 5km/h. The simulator is equipped with four dual wheel modules. The distance between the two wheels of a given module, and the distance between two different modules is as large as possible so that the wheels and gears interaction are minimized in the deepest layer of the pavement. This is done in order to study the influence of each module and each wheel on the pavement independently. As a result, the wheel track is 1550 mm, and the axle-to-axle distance between two neighboring modules is 5000 mm.

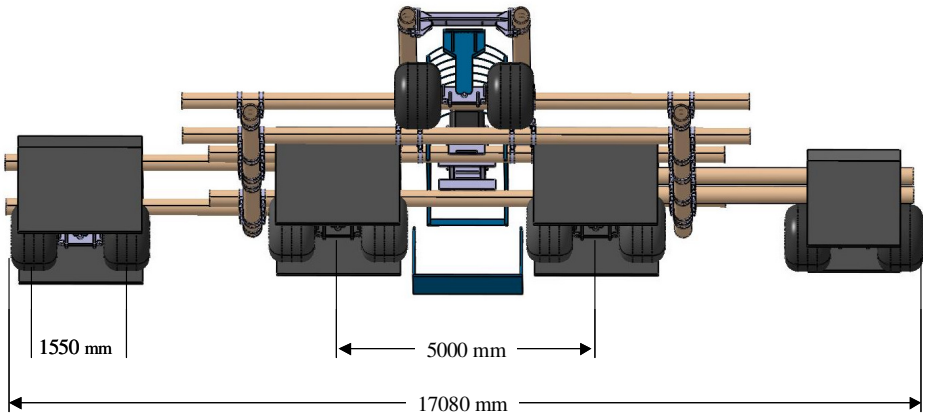

Figure 2: Simulator geometrical specification

3.2.2 Loading cases

3.2.2.1 Principle

The modular configuration of the simulator allows simulation of two different loads and two different tire pressures simultaneously, i.e. in the same meteorological and thermal conditions. The loading cases principle is represented in Figure 3. As shown in this figure, the modules M1 and M4, and M2 and M3 are identically loaded but differ in tire pressures, allowing analysis of pressure effects on the pavement. Such load repartition respects the symmetry of the simulator thus ensuring its stability. Modules M1 and M3, and M2 and M4, present identical internal tire inflation, with different loads, allowing observation and analysis of the load effect.

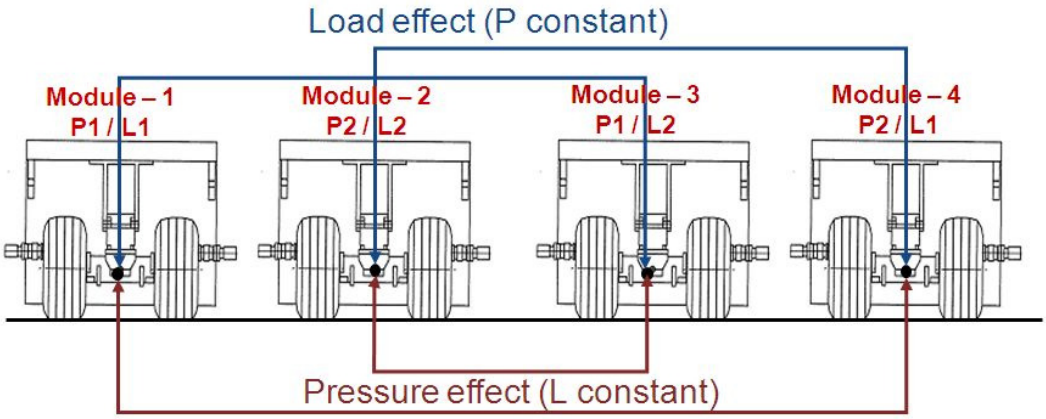

Figure 3: Loading case principle

3.2.2.2 Consolidation phase: Configuration C0

The purpose of the consolidation phase is to cover equally the whole pavement's surface with the simulator's wheels. To reach this objective, 13 different trajectories have been defined (T1 to T13) One trajectory corresponds to two passes (one in each direction) of the simulator on a given lateral position on the pavement. The lateral wandering between two consecutive trajectories is 400mm. One cycle is constituted by 26 trajectories, from T1 to T13, then from T13 to T1, each being passed on twice by the simulator (once in each direction). A cycle corresponds then to 52 passes of the simulator.

Module	Pnz[2]		Load per wheel		Deflection	Gross contact area	Passes
	Bar	PSI	Tonnes	Lbs	mm	cm²	Number
All	8.7	126	19.2	42300	123	2165	1 - 380

Table 3: Configuration C0

3.2.2.3 Fatigue Tests : Configuration C1, C2 & C3

Configuration C1, used for the first 1000 passes, and divided into two sub-configurations C1' and C1", aims at verifying the sensors' response, while applying a low load on the pavement. As a result, configuration C1' is the same as configuration C0 (used for the consolidation phase), but the wandering procedure is the one applied for all fatigue test configurations. This configuration, presented in Table 4, is used for the first 100 passes.

Module	Pnz		Load per wheel		Deflection	Gross contact area	Passes
	Bar	PSI	Tonnes	Lbs	mm	cm²	Number
M1	8.7	126	19.2	42300	123	2165	From
M2	8.7	126	19.2	42300	123	2165	1
M3	8.7	126	19.2	42300	123	2165	to
M4	8.7	126	19.2	42300	123	2165	100

Table 4: Configuration C1'

For configuration C1", and for the following configurations, the same loading process is applied. Also, tire pressures P1 and P2 are defined as P1=17.5bar and P2=15.0bar, which remains unchanged until the end of the tests. Loads applied on central modules M2 & M3, which correspond to the instrumented lines, are higher than those on external modules (L2>L1). L2 is determined using the criterion of iso-deflection of the tire (in mm) between P2=15bar and L1=19.2t onM4, and P1=17.5bar and L2 on M3 (L2 is the load for which tire deflection is the same as for tire loaded at L1 and inflated at 15 bar). Configurations of modules M1 and M2 correspond respectively to P1/L1 and P2/L2, for the comparison iso-load and iso-pressure. Results of these calculations are presented in Table 5. 900 passes have been performed in configuration C1".

Module	Pnz		Load per wheel		Deflection	Gross contact area	Passes
	Bar	PSI	Tonnes	Lbs	mm	cm²	Number
M1	17.5	254	19200	42300	72	1076	From
M2	15.0	218	22000	48500	85	1478	101
M3	17.5	254	22000	48500	80	1267	to
M4	15.0	218	19200	42300	80	1256	1000

Table 5: Configuration C1"

Highest configuration C3

The load to apply on the lightest module of configuration C3 (P2=15.0bar and L1) is derived from the tire ratings given by Michelin, namely P=17.2bar and L=34.0t at a deflection of 32%. Using the tire

[2] Internal tire pressure inflation of the loaded tire

ratings to maintain the design operating conditions (Static Load Radius) of the tire (as recommended by Michelin) at a tire pressure of 15bar, the figures obtained are P2=15bar and L1=28.7t. L2 is then determined by using the criterion of tire's iso-deflection (in mm) between P2=15bar and L1=28.7t on M4, and P1=17.5bar and L2 on M3. Configurations of modules M1 and M2 correspond respectively to P1/L1 and P2/L2. Results of these calculations are presented in Table 6.

Module	Pnz		Load per wheel		Deflection	Gross contact area	Passes
	Bar	PSI	Tonnes	Lbs	mm	cm²	Number
M1	17.5	254	28700	63270	99	1608	From 2001
M2	15.0	218	33200	73200	125	2171	
M3	17.5	254	33200	73200	112	1861	
M4	15.0	218	28700	63270	112	1877	

Table 6: Configuration C3

Intermediate configuration C2

The aim of the intermediate configuration is to progressively reach the maximum load for which the tests are performed.

The mean of L1 values of configurations C1" and C3 gives L1 value for configuration C2, i.e. L1=24.0t. L2 is determined by using the criterion of the tire's iso-deflection (in mm) between P2=15bar and L1=24.0t on M4, and P1=17.5bar and L2 on M3. L2=27.7t obtained with the iso-deflection criterion also corresponds to the mean of L2 values of configurations C1" and C3.

Configurations of modules M1 and M2 are derived from these results and correspond respectively to P1/L1 and P2/L2. This configuration, presented in Table 7, is used for 1000 passes.

Module	Pnz		Load per wheel		Deflection	Gross contact area	Passes
	Bar	PSI	Tonnes	Lbs	mm	cm²	Number
M1	17.5	254	24000	52900	84	1345	From 1001 to 2000
M2	15.0	218	27700	61100	107	1812	
M3	17.5	254	27700	61100	97	1553	
M4	15.0	218	24000	52900	97	1570	

Table 7: Configuration C2

Tire contact area is often represented as an ellipse with a uniform tire pressure distribution in the contact area. This representation is convenient for modelling related to pavement design, but not accurate when testing and simulating tire pressure effect on pavement surface course. Therefore, all loading cases tested was both simulated by using tire manufacturer models and measured by the mean of specific devices (Tekscan)

3.2.2.4 Effect of tire deflection

Under inflated conditions lead to use the tire with a lower deflection in comparison to its nominal conditions. As a direct effect, ground contact area increase and average contact pressure as well as internal tire pressure decrease (between 7.9 & 9.1%). However contact pressure distribution remains quite similar.
But, over deflection (or under inflated conditions) lead to tire life reduction, decrease rolling resistance and can lead to undesirable possible tire / brakes interactions (e.g., 0.5G turn).

3.2.2.5 Tire pressure distribution

The mean pressure in the contact area Pz (Z/NA) is a function of the unloaded tire inflation pressure Pn_0. This pressure distribution is about the same for all radial tire sizes and varies as follow (Figure.3):
$0 < Pz < 1.3 \times Pn_0$ (Tread Rib 3 Center) up to
$Pz = 2.2 \times Pn_0$ (Tread Rib 1, Shoulders) and can peak up to $2.5 \times Pn_0$ in some areas.

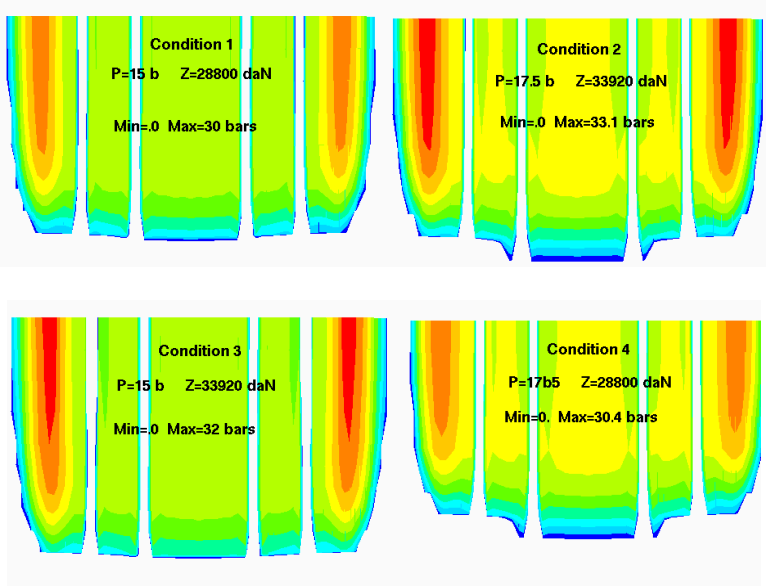

Figure 4: Calculated contact patch pressure distribution for tire size 1400x530R23 40PR at 32% deflection

The evolution of the maximum pressure is more correlated with the load level than with the inflation pressure, in this case, around this deflection point it is about: (Pmax 2 / Pmax 1 %) ~ ½ (L2 / L1 %)
The maximum pressure in the contact patch is close to 2 times the inflation pressure.
At a given load of 29.4 t (64.8 Klbs), the increase of max contact pressure observed between 15 bar and 17.5 bar is about 1.33%
At a given load of 34.5 t (76 Klbs.), the increase of max contact pressure observed between 15 bar and 17.5 bar is about 3.4%.

3.3 Instrumentation

The main objective of the instrumentation is to obtain a comprehensive description of the pavement behavior during tests.

This includes:

- ✓ Permanent component of vertical displacement of surface layers (surface layer rutting sensors)
- ✓ Horizontal resilient strains in the different asphalt layers of the structure (strain gauges)
- ✓ Vertical resilient strains in unbounded layers (strain gauges)
- ✓ Permanent component of the vertical displacement of whole pavement structure (anchored deflectometer)
- ✓ Temperature profiles in asphalt material

This aim was to provide:

- ✓ Information on the origin of rutting observed at the pavement surface
- ✓ Comparative data between configurations at 15 bar and 17.5 bar
- ✓ Absolute data for the assessment of theoretical models
- ✓ Information on temperature gradient (asphalt being sensitive to high temperature)

Section B is the reference section because EB14-BBA C thickness (8cm) is the conventional average thickness. Therefore it is the most instrumented section (see section B instrumentation plan in Figure 5).
Instrumentation is positioned along lines corresponding to wheels axle of the simulator. L2S line is the reference trajectory (15 bar modulus trajectory) and therefore the most instrumented line. L3N is the reference trajectory to 17.5 bar modulus and surface layer rutting sensors were installed to compare pressure effect.
For redundancy 3 profiles are instrumented in asphalt material and granular layer on section B and L2S line. These profiles are used to follow surface rutting evolution during tests.
L2S trajectory on sections A and C are instrumented to get comparison between two thicknesses with the same material thickness effect.
L2S trajectory on sections D and B are instrumented to get comparison between two materials with same thickness.

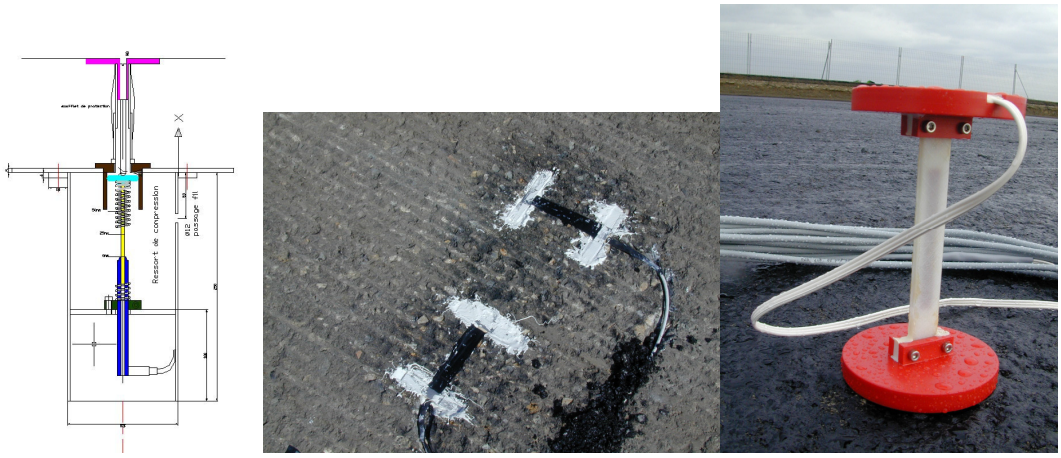

Surface layer rutting sensor Horizontal strain gauges Vertical strain gauges

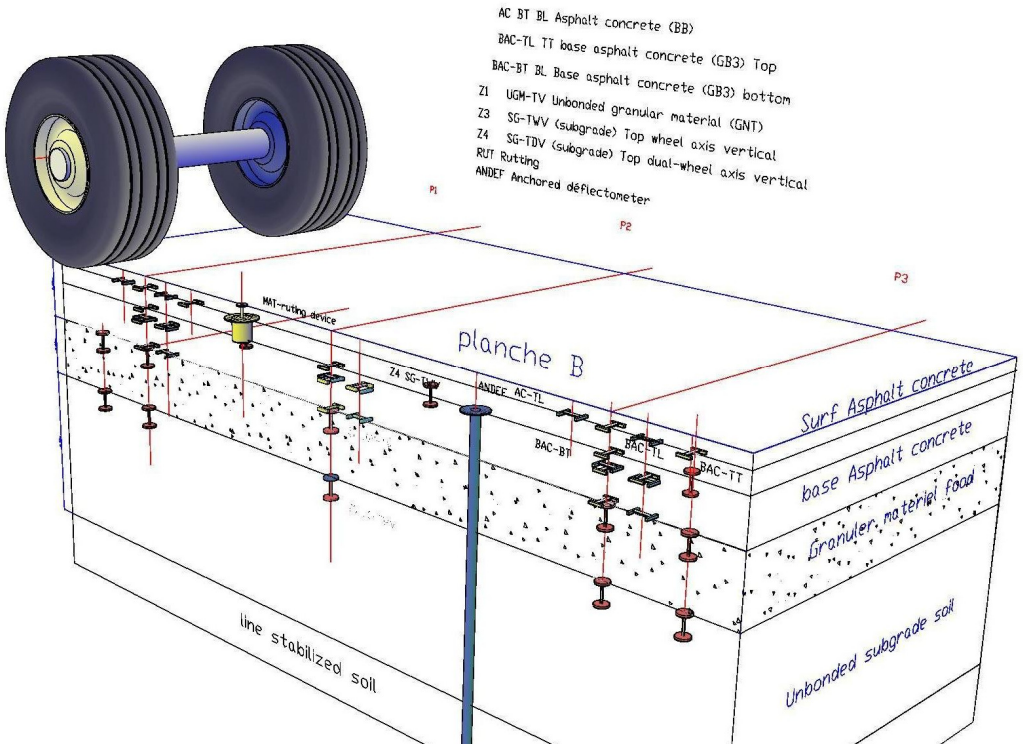

Figure 5. Instrumentation principle (Section B)

4 Test procedure

Figure 6 shows the wandering procedure selected during fatigue tests, and represents the trajectories followed by each module of the simulator. The lateral wandering between two following trajectories is 400mm. This lateral wandering aims at avoiding the creation of gutters, which would have appeared if the simulator had passed solely on trajectory "0" (i.e. the central trajectory).
Four reference lines (L1 to L4) have been defined as the trajectories followed by the axle of each module when the simulator passes on the central trajectory. For example, L1 represents the trajectory followed by the axle of module M1 when on central trajectory.
When the simulator follows trajectory "0", the external wheel of module M3 is on the instrumented line L3N, and the external wheel of module M2 is on the instrumented line L2S, as it was for the consolidation phase trajectory T7. For that reason, this central trajectory is repeated two times.
One complete cycle described 20 passes of the simulator (10 in each direction).

5 Preliminary analysis

No significant rutting or pavement evolution observed at present (end December 2009) therefore only the very first and partial analysis of the experimental results can be presented in this section.

5.1 Thermal conditions of the tests

The temperature conditions in AC surface layers during the 3 000 load applications performed today are shown in figure 6. The temperatures considered by these 4 histograms are the mean temperatures over the 8 cm AC at the top of the pavement. These are representative of common thermal condition in Southwest part of France during October to December period. The quasi-absence of rutting during these first 3 thousand loadings can be explained by the low AC temperatures. It has never exceeded 21°C, and 97% out of 3 000 loading were applied during AC mean temperature of less than 17°C.

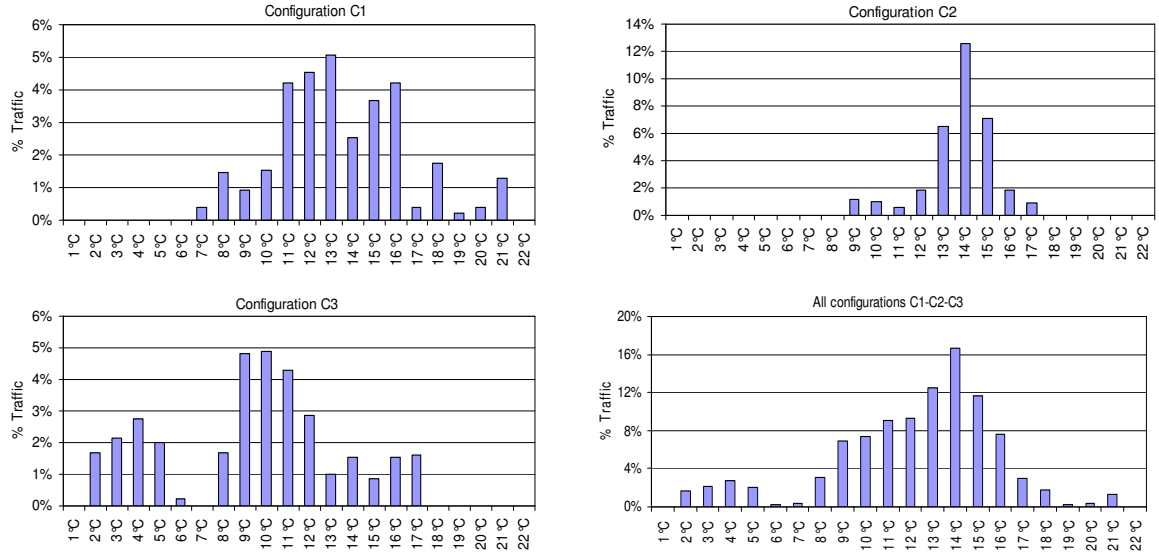

Figure 6: Temperature conditions in AC during the 3 000 first loadings

5.2 Rutting deformation at 3 000 loadings

The quasi-absence of rutting after 3 000 loadings is illustrated by figure 7 relative to the structure C (high rutting performance AC) and figure 8 relative to structure G (low rutting performance AC). These 2 figures present typical transversal profiles across the module M2 wheel-path, measured by the LRT numerical transverso-profilometer (measured width = 4.9 metres). Six level survey profiles distributed from the beginning to the 3 000 loading point are shown.

Each rutting survey operation consists of 84 transversal profiles monitors, distributed over the 7 structures and 4 twin-wheel modules (3 profiles for each structure-module set). Rutting surveys for other structures and modules are very similar to the two examples in figure 7 and 8. All of them show that the rutting depth obtained after 3 000 simulator passes is negligible. The maximum value is 1.5 mm, which corresponds to the accuracy of the LRT profilometer. Moreover, neither the load characteristics (wheel weight and tire pressure), nor the quality of the AC surface layer has any measurable influence on the rutting development.

As said before, the low temperature condition at Toulouse-Blagnac airport during the first 3 thousand loadings explains the absence of AC rutting observed up to this point, and consequently the apparently low effects of weight and tire pressure. But these temporary observations should not be extrapolated to the next stages of the test with less favourable temperatures and heaviest load & tire pressure configuration.

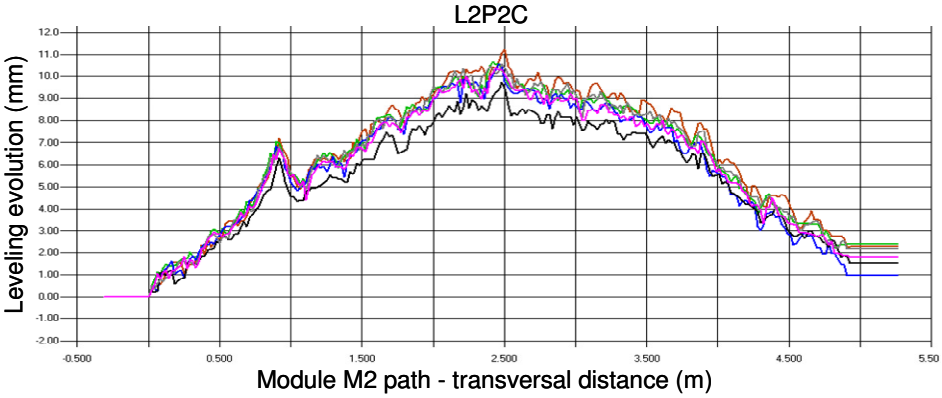

Figure 7: Structure C, module M2 path: rutting survey from 0 to 3 000 loadings by mean of the LRT numerical transverso-profilometer, examples

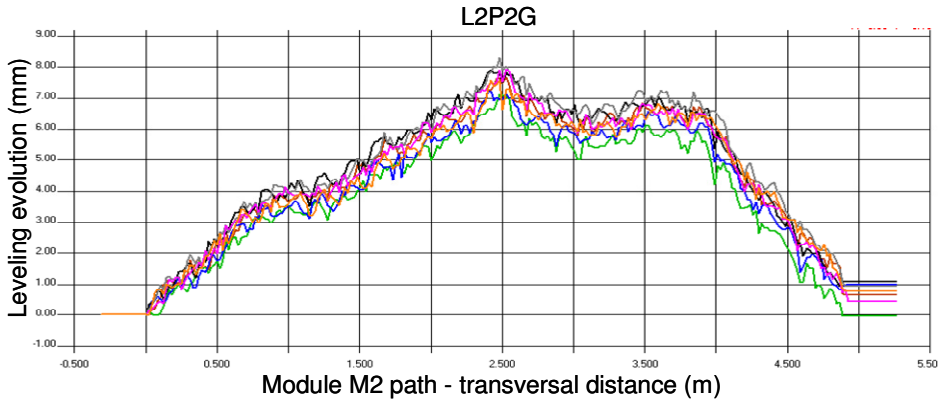

Figure 8: Structure G, module M2 path: rutting survey from 0 to 3 000 loadings by mean of the LRT numerical transverso-profilometer, examples

5.3 Tire-pavement contact pressure distribution

For load configurations C1, C2 and C3, tire footprint and the tire-pavement vertical pressure distribution are measured by the Tekscan system as presented in previously (cf. §3.2.2.5). The Tekscan sensors capture the tire footprint pressure patterns statically and/or dynamically in real time, leading to a contact pressure chart as presented in figure 9 (load 33.2 tons per wheel, inflation pressure 1.5 MPa and 1.75 MPa).

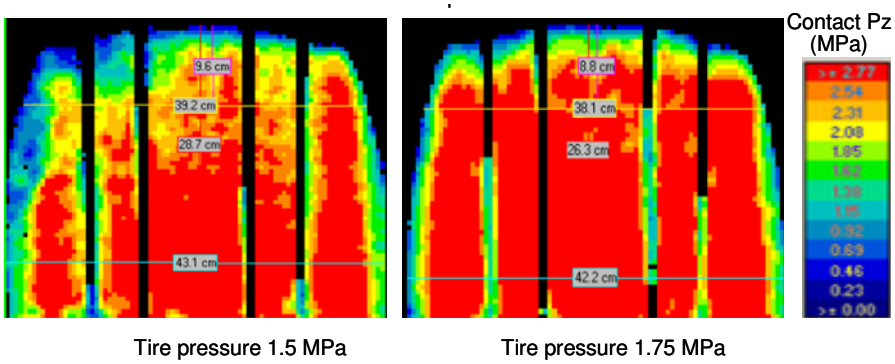

Figure 9: Vertical contact pressure pattern measured by the Tekscan system
(example for configuration C3, 33.2 tons per wheel, 1.5 and 1.75 MPa)

In order to accurately quantify the effects of tire inflation on the tire/pavement contact pressure distribution, 2 transversal contact pressure profiles are derived from these charts: the median transversal profile P1 and the edge transversal profile P2 (distance from P2 = A/3, with A=total footprint length). The vertical contact pressure variations along profiles P1 and P2 for the same load characteristics are shown in figure 10 and figure 11. Table 8 reproduced the overall length (=A) and width (=B) of the footprint, according to the inflation tire pressure.

	Configuration C3 – 33.2 t/wheel	
	Tire pressure 1.5 MPa	Tire pressure 1.75 MPa
Length A (cm)	57.4	52.6
Width B (cm)	43.1	42.2
Mean vertical contact pressure (MPa)	1.32	1.46

Table 8: Tire footprint dimensions – load configuration C3,
measured by the Tekscan system

Table 8 and figures 10-11 lead to the following observations:

- The tire pressure mainly influences the footprint length: -9% decrease in length A against -2% decrease in width B, as tire pressure increases from 1.5 to 1.75 MPa.
- The vertical tire/pavement contact pressure distribution appears to be nearly symmetrical in relation to the wheel longitudinal axis. In the contact area centre (cf. profile P1), the tire pressure increase induces a nearly uniform contact pressure increase over the whole footprint width print. But near the footprint edges (cf. profile P2) the central region of the contact area is not affected by the tire pressure increase.
- Very high values of the vertical contact pressure are locally observed: 4 MPa and 5 MPa respectively for the tire pressure 1.5 and 1.75 MPa. Increase in maximum contact pressure value is +7%, as inflation pressure increase is +17%.
- Given these considerable values (4 and 5 MPa), there is no doubt that the mean contact pressure value (1.32 and 1.46 MPa, cf. table 8) is not an appropriate input data for stress and strain paths modelling the in the upper part of the pavement.
- The 2 previous experimental observations do not agree with the numerical simulations presented before in section 3 (cf. §3.2.2.5), which predict that the maximum contact pressure if not significantly affected by the tire pressure increase, contrary to the tire load. Investigations must be made in order to determine whether the tire manufacturer simulation model or the Tekscan measurement device have been over or under-estimated.

- These first tire pressure effects experimental results and conclusions are still temporary. Complementary contact pressure distribution measures will be still performed as the HTPT continue.

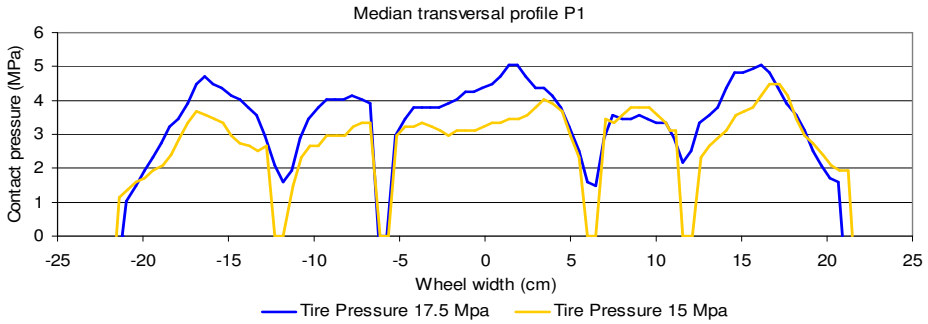

Figure 10: Vertical contact pressure variation along the transversal median profile P1 derived from the Tekscan measures. Example for configuration C3, 33.2 tons per wheel

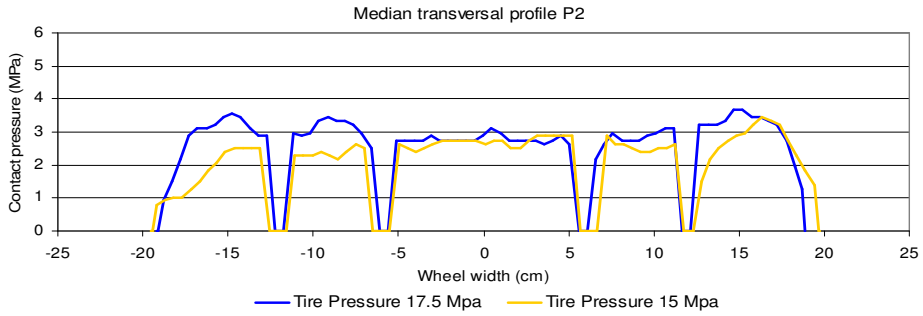

Figure 11: Vertical contact pressure variation along the edge profile P2 derived from the Tekscan measures. Example for configuration C3, 33.2 tons per wheel

For strain gauges and deflection measurement theoretical analysis, and also to estimate the effect of tire pressure on the shear stresses in the pavement material (not measured), numerical simulation including real non-uniform vertical pressure distribution applied at the surface of the pavement, must be performed. Indeed, the detailed pressure chart measured by the Tekscan system cannot be directly used as input for this computation; therefore simplified pressure patterns are needed, based on the transversal pressure profile P1 and P2.

5.4 Strain-gauge signals

From the start of testing to 1 000 loadings, a complete sensor acquisition including the recording of 116 stain-gauges and 14 LVDT sensors (130 channels valid today) is recorded at each simulator run. See §3.3 for a detailed presentation of the instrumentation. From 500 loadings to today (3 000 passes) 1 230 further data acquisitions were recorded.

These measurements constitute a database including 2 230 data acquisition at the present time, stored in 1 115 ASCII measurement files (one file for one simulator pass-and-back). Pavement temperature survey is also performed continuously (acquisition period = 15 minutes) since the beginning of the test.

This database will potentially allow a complete description of the dynamic response of the experimental pavement trafficked by heavy loads at low speed under variable thermal conditions. However, it should be observed that the pavement instrumentation was initially conceived for a typical

and new airport runway without anticipating subsequent reinforcement (cf. §3.1.5). Therefore it could be concluded that an appreciable part of the instrumentation objectives will not be fully obtained by the end of the tests, mainly concerning data for the French rational design method for new airfield pavement assessment and the calibration. However full instrumentation installed in the pavement part, sensitive to tire pressure effect was entirely reproduced so that tire pressure effect on surface and base asphalt concrete can be accurately assessed.

As tests are still continuing and only low temperatures are concerned, the data analysis remains preliminary. Most important elements are related below:

5.4.1 Wearing course-base AC interface

The quality and durability of the bonding between the different pavement layers highly affect the structural resistance of the pavement. As heavy load induced very high shear stresses in the upper pavement layers, interface un-bonding of the wearing course must be considered as a possible degradation mode of the pavement, which significantly reduces its service life by developing premature cracks and accelerating subsequent deterioration.
Information concerning the bonding condition between the AC wearing course and the base AC layer may be deduced from the strain gauge response at the bottom and the top of these two layers.

Figure 12 shows typical signals measured for the load conditions C2 and C3. Contraction strains are expressed with negative sign. Flexural strains created by the load at the bottom of the AC surface and the top of the base AC layers are both contraction strain. Furthermore, the maximal contraction strain values at on both sides of the interface are very close. It clearly reveals the flexural strain vertical continuity in the structure and consequently good bonding condition between the two layers, in spite of the very high loads and tire pressure applied to the pavement.

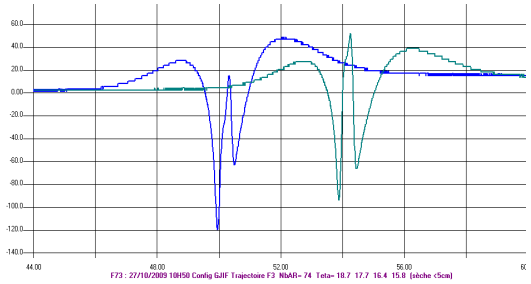

Configuration C2, Temp=17.2°C
Longitudinal stain gauge at the bottom of the surface AC: Typical signal long = f(time)

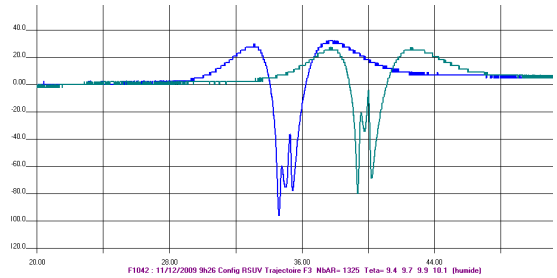

Configuration C3, Temp=9.8°C
Longitudinal stain gauge at the bottom of the surface AC: Typical signal long = f(time)

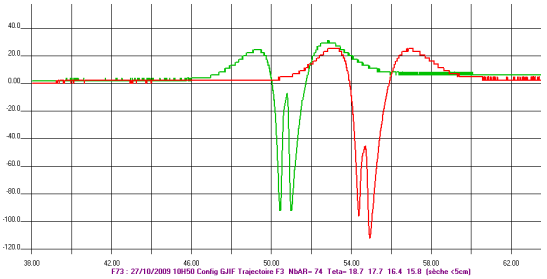

Configuration C2, Temp=17.2°C
Longitudinal stain gauge at the top of the base AC: Typical signal long = f(time)

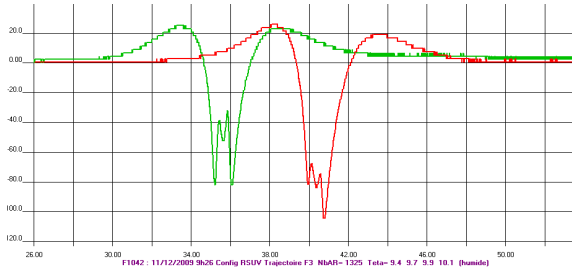

Configuration C3, Temp=9.8°C
Longitudinal stain gauge at the top of the base AC: Typical signal long = f(time)

Figure 12: Typical strain-gauge signals at the bottom of the surface AC and the top of base AC layer. Structure B, load configuration C2 and C3, tire pressure 1.75 Mpa (gauge measure in µstrain, negative sign for contraction)

5.4.2 Vertical strains gauges and vertical displacement sensors

Typical signals measured by the vertical strain gauges at the top of the UGM subbase and capping layer are presented in figure 13.

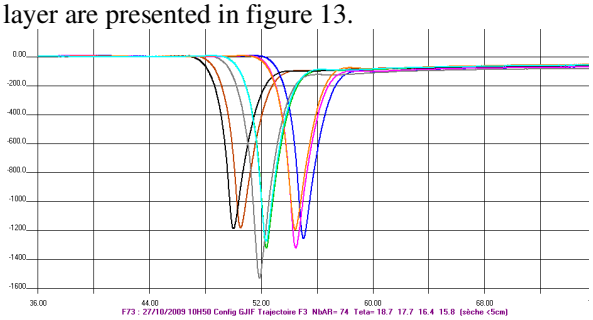

Configuration C2, Temp=17.2°C
Vertical stain gauge at the top the UGM subbase
Typical signal vert = f(time)

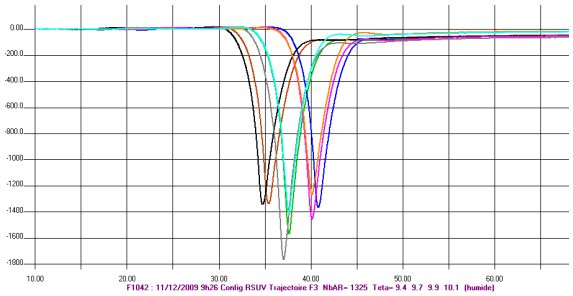

Configuration C3, Temp=9.8°C
Vertical stain gauge at the top the UGM subbase
Typical signal vert = f(time)

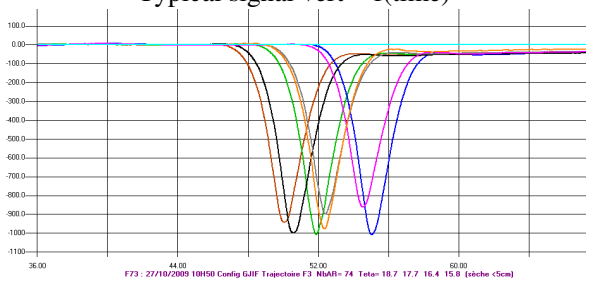

Configuration C2, Temp=17.2°C
Vertical stain gauge at the top the UGM capping layer
signal vert. = f(time)

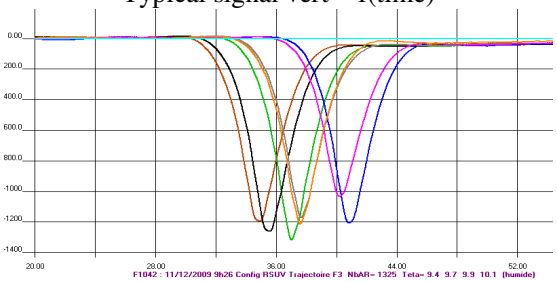

Configuration C3, Temp=9.8°C
Vertical stain gauge at the top the UGM capping layer
signal vert = f(time)

Figure 13: Typical strain-gauge signals at the top of the UGM subbase and the top of UGM capping layer. Structure B, load configuration C2 and C3, tire pressure 1.75 Mpa (gauge measure in µstrain, negative sign for contraction)

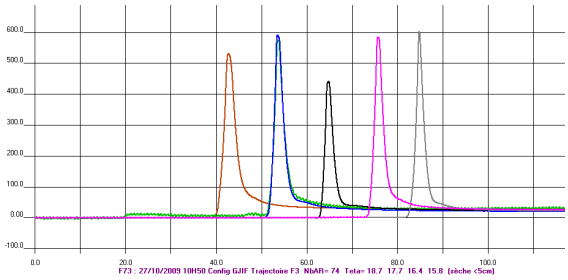

Configuration C2, Temp=17.2°C
Anchored deflectometer:
typical signal Da = f(time)

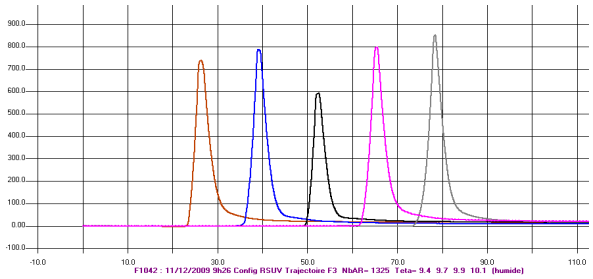

Configuration C3, Temp=9.8°C
Anchored deflectometer:
typical signal Da = f(time)

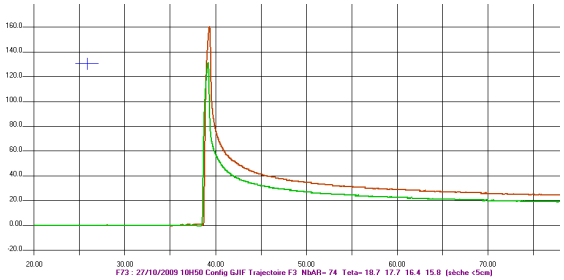

Configuration C2, Temp=17.2°C
Surface layer rutting sensor:
typical signal vert = f(time)

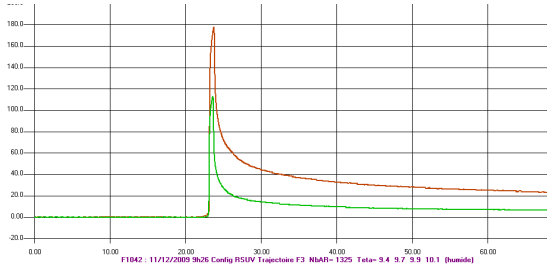

Configuration C3, Temp=9.8C
Surface layer rutting sensor:
typical signal vert = f(time)

Figure 14: Typical strain-gauge signals at the top of the UGM subbase and the top of UGM capping layer. Structure B, load configuration C2 and C3, tire pressure 1.75 Mpa (gauge measure in µstrain, negative sign for contraction)

Typical signals measured by the anchored deflectometer and surface layer rutting sensors are presented in figure 14.

Strain and displacement signals as those shown in figures 12, 13 and 14 will be analysed in a later task of the HTPT project, according to major objectives:

1- Evaluation of tire inflation pressure effects and
2- Improvement of the structural modelling of pavement under heavy load.

As both these objectives are largely based on comparisons between the sensor responses under different loads and/or tire pressures, it is important to evaluate the accuracy and the reproducibility of the various sensors, and their sensitivity to other external factors.

To evaluate if the sensors return more or less identical measures under the same loading conditions (i.e. sensor repeatability), special runs of the simulator were performed. They consist in ten successive simulator go-and-back along exactly the same median trajectory (T3). The signals measured by horizontal strain gauges at the bottom of surface AC and the top of the UGM subbase are presented on figures 15 and 16 respectively. It is observed that the mean repeatability range is about 5% (common value fort this type of pavement instrumentation). It also should be observed that this range of accuracy is close to the effect on the tire-pavement contact pressure of the increased inflation pressure from 1.5 MPa to 1.75 MPa (+7%, cf.§5.3). This leads to the conclusion that the effects of tire pressure on the pavement structural behaviour must not focus on the analysis of local and individual gauge responses. But it is essential to integrate a statistical approach taking into account the response fluctuations of the different sensors between them, and their one reproducibility characteristics.

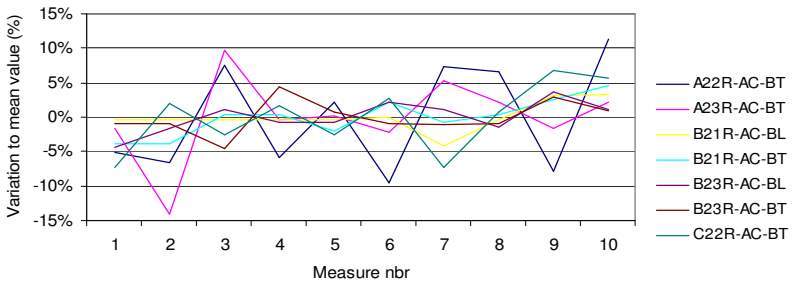

Figure 15: Sensor repeatability tests. Signals measured by horizontal strain-gauges at the bottom of surface AC

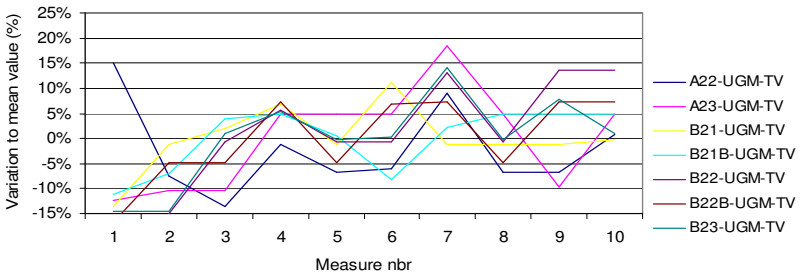

Figure 16: Sensor repeatability tests. Signals measured by horizontal strain-gauges at the top of the UGM subbase

Figure 17, 18 and present the sensitivity of strain gauges to the mean temperature in the AC materials. All gauges responses exhibit a high susceptibility to temperature condition in AC materials, which consolidate firstly the very complete temperature instrumentation and monitoring during the whole HTPT tests, and secondly the limits of focusing on local or individual gauge signal in result analysis.

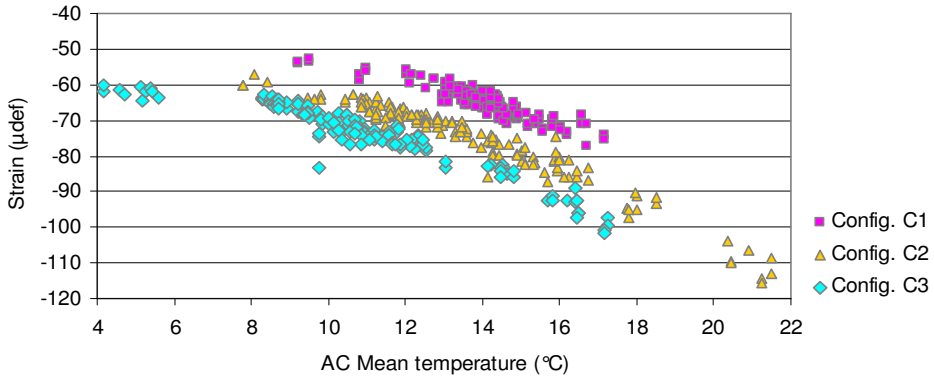

Figure 17: Maximal longitudinal strains measured at the bottom of AC surface layer - susceptibility to AC temperature

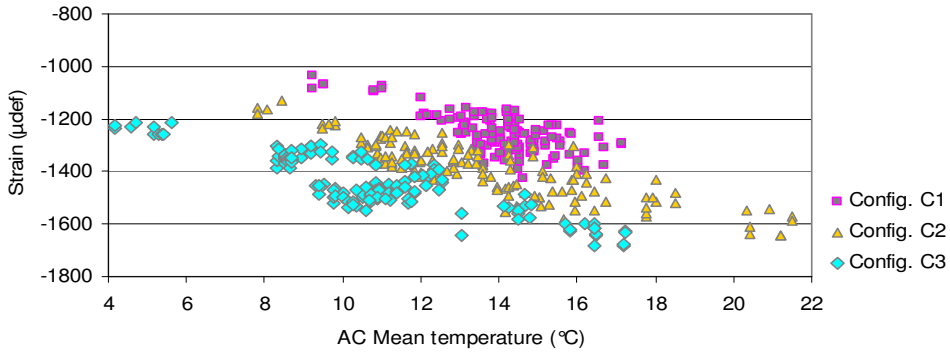

Figure 18: Maximal vertical strains measured at the top of UGM subbase - susceptibility to AC temperature

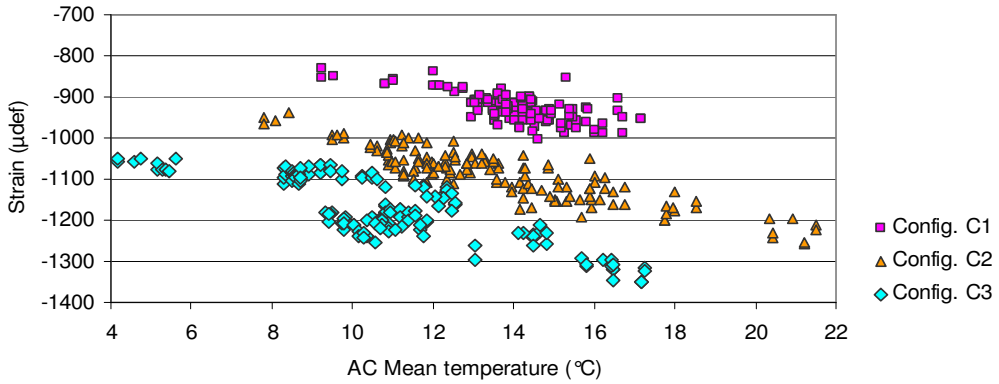

Figure 19: Maximal vertical strains measured at the top
of UGM capping layer - susceptibility to AC temperature

6 Way forward

These tests are on-going and will complete and support the Boeing tests for ICAO submission via the AOSWG, Pavement subgroup (PSG). International aviation industry representatives (FAA, BOEING, CAAs) are kept informed of test progress (one Workshop in 2009 and another one plan in June 2010 for final test conclusion and recommendations) and we would expect ICAO to take advantage of these test results to support a superior and more precise limiting tire pressure criteria methodology more in line with current and future aircraft.
Analysis will be updated continuously therefore material presented during the conference could be different and more complete than described in this paper

REFERENCES

ROGINSKY P.E, 2006, *High tire inflation pressure test on flexible pavement*
ICAO, 2004, *Aerodromes, Volume I, Aerodrome Design and operations*
ICAO, 1983, *Aerodrome Design manual, Doc 9157-AN/901 Part 3*